Measurement of through-focus EUV pattern shifts using the SHARP actinic microscope

Obert Wood, Yulu Chen, Pawitter Mangat, Kenneth Goldberg, Markus Benk, et al.

Obert Wood II, Yulu Chen, Pawitter Mangat, Kenneth Goldberg, Markus Benk, Bryan Kasprowicz, Henry Kamberian, Jeremy McCord, Thomas Wallow, "Measurement of through-focus EUV pattern shifts using the SHARP actinic microscope," Proc. SPIE 10450, International Conference on Extreme Ultraviolet Lithography 2017, 1045008 (16 October 2017); doi: 10.1117/12.2280371

SPIE.

Event: SPIE Photomask Technology and EUV Lithography, 2017, Monterey, California, United States

Measurement of through-focus EUV pattern shifts using the SHARP actinic microscope

Obert Wood[*a], Yulu Chen[b], Pawitter Mangat[a], Kenneth Goldberg[c], Markus Benk[c], Bryan Kasprowicz[d], Henry Kamberian[e], Jeremy McCord[e], and Thomas Wallow[f]

[a]GLOBALFOUNDRIES, 400 Stonebreak Rd. Extension, Malta, NY 12020 USA
[b]GLOBALFOUNDRIES, 257 Fuller Road, Albany, NY 12203 USA
[c]Center for X-Ray Optics, 1 Cyclotron Road, Berkeley, CA 94720 USA
[d]Photronics, Inc., 601 Millenium Drive, Allen, TX 75013 USA
[e]Photronics, Inc., 10136 South Federal Way, Boise, ID 83716 USA
[f]ASML Brion Technologies, 4211 Burton Drive, Santa Clara, CA 95054 USA

ABSTRACT

This paper provides experimental measurements of through-focus pattern shifts between contact holes in a dense array and a surrounding pattern of lines and spaces using the SHARP actinic microscope in Berkeley. Experimental values for pattern shift in EUV lithography due to 3D mask effects are extracted from SHARP microscope images and benchmarked with pattern shift values determined by rigorous simulations.

Keywords: EUV, 3D mask effects, pattern shift, rigorous 3D mask lithography simulation.

1. INTRODUCTION

This paper provides experimental measurements of the through-focus relative pattern shift between contact holes in dense contact-hole arrays and a surrounding pattern of lines and spaces on an EUV reflective mask extracted from actinic images of these patterns captured with the SHARP actinic microscope in Berkeley [1]. Because the reflective masks utilized by EUV lithography must be illuminated at an oblique angle in order to separate incident and reflected light, the coating structure on an EUV mask has an inordinately large impact on wafer image quality and gives rise to a variety of 3D mask effects including horizontal-vertical print differences, a diffraction imbalance in the pupil of the imaging system, and through-focus pattern placement (telecentricity) errors on printed wafers. In the past, the magnitude of 3D mask effects has been examined experimentally using images of EUV masks captured with the SHARP actinic microscope [2], using mask diffractometry data collected with the EUV reflectometer on Physikalisch-Technische-Bundesanstalt (PTB's) soft x-ray radiometry beamline at the BESSYII synchrotron in Berlin, and at the wafer-level by measuring the relative shift between two sets of line and space patterns printed using EUV lithography using CD-SEM metrology [3]. Even so, since almost all of what is known about EUV 3D mask effects have come from simulations carried out using commercially-available, rigorous mask 3D simulators, e.g., S-Litho (Synopsys) [4], the need for additional benchmarking of the simulations with measurement data is increasingly critical.

Since extreme ultraviolet (EUV) lithography at 13.5 nm wavelength is a potential patterning technology for high volume manufacturing of semiconductor devices at the 7 nm technology node and beyond, each of the techniques known to mitigate EUV 3D mask effects, including application of optical proximity corrections (OPC) to the geometric layout of the mask patterns to pre-correct the image deformations [5], utilization of a number of innovative source-mask optimization (SMO) resolution enhancement techniques [6-7], and development of EUV masks with alternatives to the conventional Ta-based absorber Mo/Si multilayer reflector film stack [8-9], needs to be benchmarked to experimental measurement data.

[*] obert.wood@globalfoundries.com; phone 1 518 305-7809

International Conference on Extreme Ultraviolet Lithography 2017, edited by Paolo A. Gargini, Patrick P. Naulleau, Kurt G. Ronse, Toshiro Itani, Proc. of SPIE Vol. 10450, 1045008

2. EUV MASK & MASK METROLOGY

The EUV test mask used for the through-focus pattern shift measurements described in this paper was fabricated at Photronics, Inc. in Boise Idaho on an EUV mask blank from Hoya Corporation with a Ru-capped Mo/Si multilayer with 40 bilayers overcoated with an absorber consisting of 58 nm of TaBN and an anti-reflection coating (ARC) consisting of 2 nm of TaBO on a ULE substrate. The Ta-based absorber was patterned with dense contact hole arrays at 80, 64 and 56 nm pitch surrounded by coarse line & space patterns at 240, 172 and 162 nm pitch which served as fiducials when extracting relative pattern shift information. A diagram of the mask pattern for the 56 nm pitch contact hole array surrounded by the 162 nm pitch line & space fiducial array is shown in Figure 1(a).

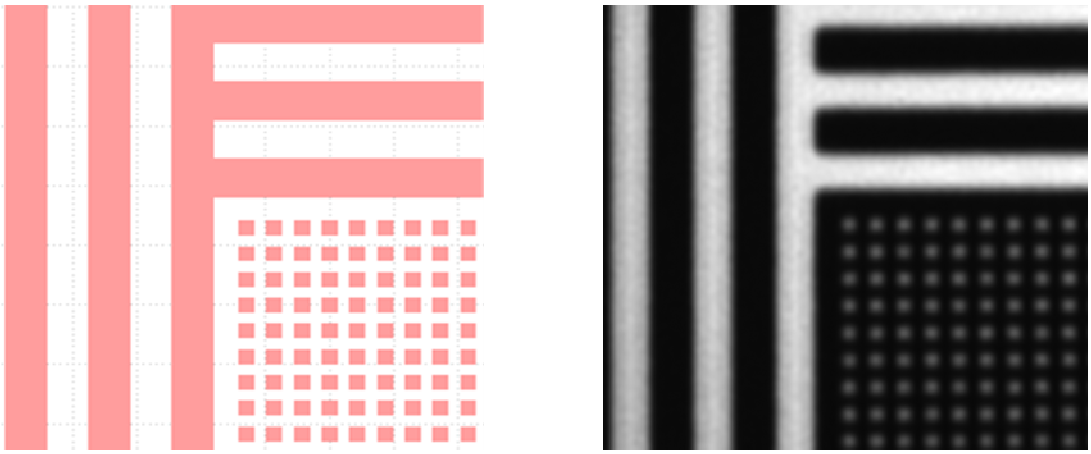

(a) (b)

Figure 1 (a) Diagram of mask pattern for dense contact-hole array and surrounding line and space pattern and (b) actinic image of corresponding area on an EUV mask captured with the SHARP actinic microscope.

An actinic EUV image of an orthogonal 54 nm pitch contact-hole array and surrounding line and space pattern illustrated in Figure 1(a) captured using the SHARP microscope at 0.33 NA using Quasar 45 illumination at 13.5 nm wavelength is shown in Figure 1(b). The SHARP microscope uses off-axis Fresnel zoneplate lenses to project near diffraction-limited EUV images of photomask patterns onto a 1-inch EUV CCD detector at 900x or higher magnification. EUV radiation produced by the storage ring at the Advanced Light Source in Berkeley illuminates a small region on the mask, and a zoneplate lens, selected among 4xNA values from 0.25 to 0.625, captures the reflected light and projects it directly upward to the CCD, a distance of approximately 450 mm above the mask surface. SHARP's Fourier-synthesis illuminator can create disk, annular, dipole, quadrupole, quasar, cross-pole and other custom illumination patterns. For this paper, the actinic images were captured with quasar 45 illumination, with inner/outer sigma settings of 0.2/0.9, and a zone plate lens with a NA of 0.33 to emulate the imaging properties of current 0.33 NA EUV lithography tools, albeit only over a small field of view (30 µm FOV and ~5-µm diffraction-limited central region). The SHARP microscope is capable of navigating the entire active area of an EUV mask and can record approximately 20 through-focus series of actinic images per hour.

3. DATA ANALYSIS

A through-focus series of 17 actinic images of the patterns shown in Figure 1(a) were recorded at 200 nm step size (equivalent to 25 nm at wafer scale) with the SHARP actinic microscope. Preprocessing of the SHARP data, which consisted of alignment, rotation and export to tiff file format, was done using custom image processing software called ThroughFocus 3 from Kanayama Consulting. The actinic images were subsequently separated into three parts—contact holes, horizontal lines, and vertical lines, as shown in Figure 2.

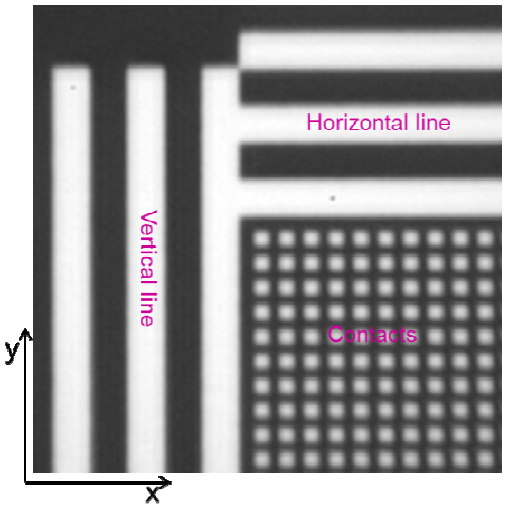

Figure 2 Sketch illustrating how values for relative pattern shift between the x/y positions of the horizontal and vertical lines and the individual contacts in the dense array were determined.

Centroids for 100 contact holes closest to the lines were determined by the Matlab 'regionprops' function. The horizontal and vertical lines were decomposed into multiple segments and centroids were extracted for each segment before a linear fit was performed to determine the line position. The process was repeated for 7 of the through-focus images near best focus and the values for the relative shift of the contact holes with respect to the lines were determined and plotted in Figure 3 after converting all numbers to wafer scale, by dividing defocus values by 16 and length values by 4, and converting pixel values to nm (1 pixel = 2.5 nm, wafer scale). Error bars in Fig. 3 represent the standard deviation ($\pm\sigma$) of the shifts of 100 contact holes with respect to the lines.

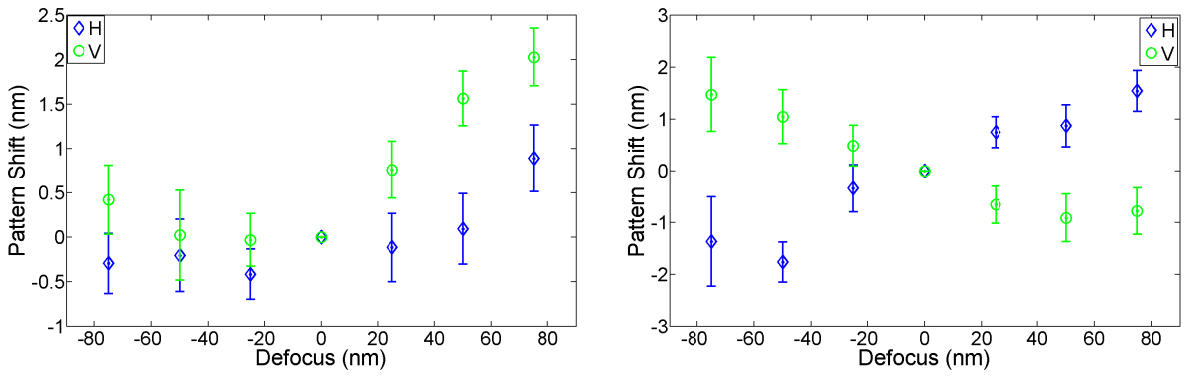

Figure 3 Pattern shift measurement data from two sets of actinic images captured with the SHARP microscope by changing the focus of the 0.33 NA zone plate lens via mechanical stage motion (a) and by scanning the EUV illumination wavelength (b).

Through-focus series of actinic images were recorded with the SHARP microscope in Berkeley by physically moving the 0.33NA Fresnel zoneplate lens that projects an image of the illuminated mask surface onto an EUV detector, towards or away from the mask surface with a precision mechanical stage (as shown in Figure 3(a)) or by changing the focus of the zone plate lens by changing the EUV illumination wavelength (as shown in Figure 3(b)). Because of its narrow band illuminator, SHARP can change the focus of the zoneplate lens by wavelength tuning over a narrow range near 13.5 nm wavelength, from approximately 13.2 to 13.7 nm, since with Fresnel zoneplate lenses the product of wavelength (λ) and focus (f) is constant [10]. A comparison of the pattern shift data reproduced in Figures 3(a) & 3(b) shows that the pattern shift values recorded when defocus was produced with a stage motion are much less accurate than pattern shift values recorded when defocus was produced by wavelength tuning. This is partially due to the inability of the zoneplate

stage to take consistent and accurate steps. We suggest that accurate through-focus measurements of pattern shift with the SHARP microscope should always be captured when defocus is produced by wavelength tuning.

4. DISCUSSION

Because through focus pattern shift is fundamentally caused by the imbalance of diffraction order intensity, more isolated structures will have smaller pattern shifts as less light is absorbed by the mask absorber. In Fig. 4, we show extracted pattern shifts through focus for contact arrays with different pitches, 80nm x 80nm in Fig. 4(a) and 56nm x 56nm in Fig. 4(b). It can be clearly observed that the pattern shifts for the more isolated pitch contact array is consistently smaller than the pattern shifts for the dense contact array, in agreement with theory.

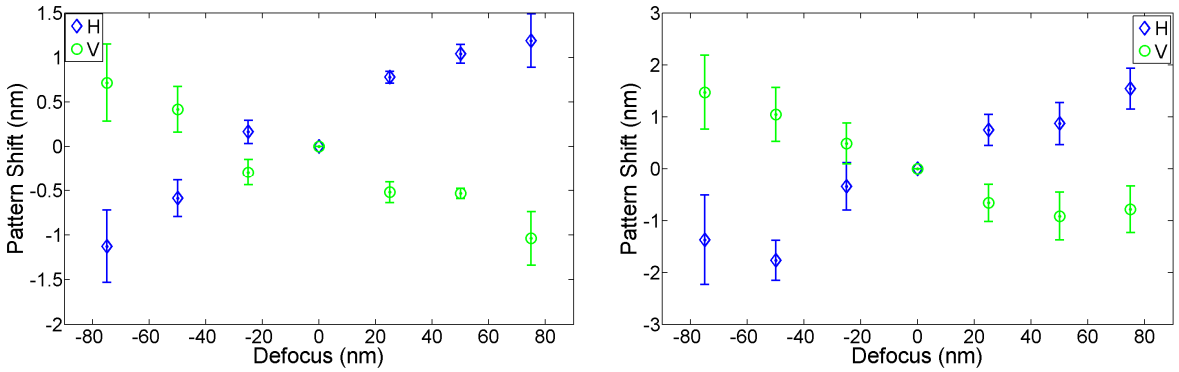

Figure 4 Through focus pattern shifts for contact arrays with different pitches, (a) 80nmx80nm and (b) 56nmx56nm.

Comparison of measured (data points with error bars) and simulated (solid lines) relative pattern shift between individual 56 nm pitch contact holes in a dense contact hole array and a surrounding line and space pattern fiducial as a function of defocus determined from a through-focus series of mask images captured with the actinic SHARP microscope in Berkeley is shown in Figure 5.

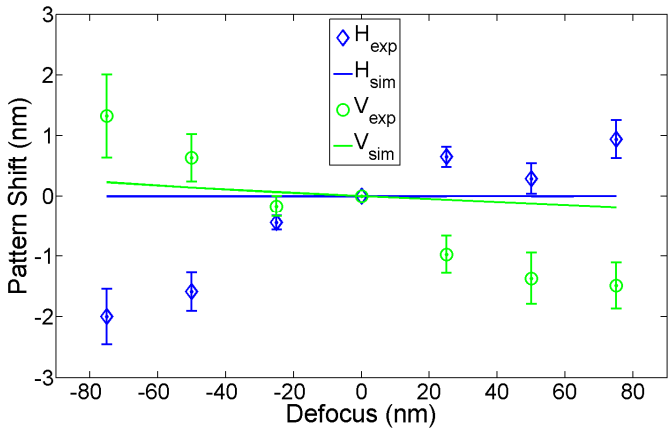

Figure 5 Comparison of measured (data points with error bars) and simulated (solid lines) relative pattern shift between individual contact holes in a dense contact hole array and a surrounding line and space pattern fiducial as a function of defocus determined from a through-focus series of mask images captured with the actinic SHARP microscope in Berkeley.

Since the EUV mask pattern was illuminated at 6° to the mask normal in the vertical direction (central ray is in the y-z plane), the image shift in the horizontal direction should have been exactly zero. The measurement data in Figure 5 shows that the experimental values in the horizontal direction are decidedly not zero. The experimental values for pattern shift in the horizontal direction are ~6x larger (approximately 0.019nm pattern shift per nm defocus for both

directions) than the values predicted in the simulation. Possible reasons for the discrepancy between measurement and simulation could be a) the method used to locate the contact hole centroids needs improvement, and b) the zone plate lenses in the actinic microscope have much larger than expected aberrations. Both explanation seem unlikely since a recent attempt to measure directly the 3-order aberration in the SHARP zoneplate lenses at 0.25 and 0.33 NA using an image-based technique [11] reported values for 3rd order Zernikes of 63.6 milliwaves, i.e., considerably smaller than those needed to match the simulation values. At a minimum, the experimental measurements plotted in the figure provide an upper limit to the magnitude of the relative pattern shift due to EUV 3D mask effects.

5. CONCLUSIONS

The SHARP actinic microscope in Berkeley was used to image the through-focus pattern shift between contact holes in a dense contact-hole array and a surrounding pattern of lines and spaces on an EUV test mask caused by 3D mask effects. While the correspondence between measured and simulated pattern shift values is not as close as expected, the observation of pattern shifts of 1 – 2 nm provides an upper limit for their magnitudes. The measurements of through focus pattern shift using the SHARP actinic microscope show that the pattern shift values recorded with SHARP when defocus was produced with a mechanical motion of the zoneplate lens were considerably noisier that the pattern shift values recorded with SHARP when defocus was produced by wavelength tuning.

REFERENCES

[1] Goldberg, K., Benk, M., Wojdyla, A., Mochi, I., Rekawa, S., Allezy, A., Dickinson, M., Cork, C., Chao, W., Zehm, D., Macdougall, J., Naulleau, P., Rudack, A., "Actinic mask imaging: Recent results and future directions from the SHARP EUV microscope," Proc. SPIE **9048**, 90480Y (2014).

[2] Raghunathan, S., Wood, O., Mangat, P., Verduijn, E., Philipsen, V., Hendrickx, E., Jonckheere, R. Goldberg, K., Benk, M., Kearney, P., Levinson, Z., Smith, B.W., "Experimental measurements of telecentricity errors, in high-numerical-aperture extreme ultraviolet mask images," J. Vac. Sci. Technol. B. **32**, 06F801 (2014).

[3] Philipsen, V., Hendrickx, E., Verduijn, E., Raghunathan, S., Wood, O., Soltwisch, V., Scholze, F., Davydova, N., Mangat, P., "Imaging impact of multilayer tuning in EUV masks, experimental validation," Proc. SPIE **9235**, 92350J (2014).

[4] http://www.synopsys.com/Tools/Manufacturing/MaskSynthesis/Pages/Sentaurus-Lithography.aspx.

[5] Erdmann, A., Xu, D., Evanschitzky, P., Philipsen, V., Luong, V., Hendrickx, E., "Characterization and mitigation of 3D mask effects in extreme ultraviolet lithography," Adv. Opt. Techn. **6**, 187 (2017).

[6] Hsu, S., Howell, R., Jia, J., Liu, H-Y, Gronlund, K., Hansen, S., Zimmerman, J., "EUV resolution enhancement techniques (RETs) for k_1 0.4 and below," Proc. SPIE **9422**, 94331I (2015).

[7] Kim, R.-H., Wood, O., Crouse, M., Chen, Y., Plachecki, V., Hsu, S., and Gronlund, K., "Application of EUV resolution enhancement techniques (RET) to optimize and extend single exposure bi-directional patterning for 7nm and beyond logic designs," Proc. SPIE **9776**, 97761R (2016).

[8] Wood, O., Raghunathan, S., Mangat, P., Philipsen, V., Luong, V., Kearney, P., Verduijn, E., Kumar, A., Patil, S., Laubis, C., Soltwisch, V., Scholze, F., "Alternative materials for high numerical aperture extreme ultraviolet lithography mask stacks," Proc. SPIE **9422**, 94220I (2015).

[9] Hay, D., Bagge, P., Khaw, I., Sun, L., Wood, O., Chen, Y., Kim, R.-H., Qi, Z. J., and Shi, Z., "Thin absorber extreme ultraviolet photomask based on Ni–TaN nanocomposite material." Opt. Lett. **41**, 3791 (2016).

[10] Goldberg, K.A., Mochi, I. Huh, S., "Collecting EUV mask images through focus by wavelength tuning," Proc. SPIE **7271,** 72713N (2009).

[11] Levinson, Z, Smith, B., Raghunathan, S., Wood, O., "An image-based method for EUVL aberration metrology," International Symposium on Extreme Ultraviolet Lithography, Washington, DC, 23 October 2014.